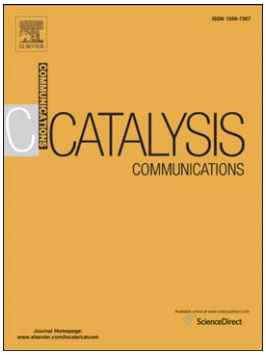

Synthesis of palladium nanoparticles on carbon nanotubes and graphene for the chemoselective hydrogenation of para-chloronitrobenzene

A.B. Dongil, L. Pastor-Pérez, J.L.G. Fierro, N. Escalona, A. Sepúlveda-Escribano

PII: S1566-7367(15)30158-8
DOI: doi: 10.1016/j.catcom.2015.12.004
Reference: CATCOM 4521

To appear in: *Catalysis Communications*

Received date: 2 September 2015
Revised date: 13 November 2015
Accepted date: 3 December 2015

Please cite this article as: A.B. Dongil, L. Pastor-Pérez, J.L.G. Fierro, N. Escalona, A. Sepúlveda-Escribano, Synthesis of palladium nanoparticles on carbon nanotubes and graphene for the chemoselective hydrogenation of para-chloronitrobenzene, *Catalysis Communications* (2015), doi: 10.1016/j.catcom.2015.12.004

Synthesis of palladium nanoparticles on carbon nanotubes and graphene for the chemoselective hydrogenation of para-chloronitrobenzene.

A.B.Dongil*[1], L.Pastor-Pérez[2], J.L.G Fierro [3], N. Escalona[4,5], A.Sepúlveda-Escribano[2]

[1] *Universidad de Concepción, Facultad de Ciencias Químicas, Casilla 160C, Concepción, Chile.*

[2] *Laboratorio de Materiales Avanzados, Departamento de Química Inorgánica- Instituto Universitario de Materiales de Alicante, Universidad de Alicante, Apartado 99, E-03080 Alicante, Spain.*

[3] *Instituto de Catálisis y Petroleoquímica CSIC, Grupo de Energía y Química Sostenible, C/Marie Curie 2, Cantoblanco, Madrid, Spain.*

[4]*Departamento de Ingeniería Química y Bioprocesos, Escuela de Ingeniería, Pontificia Universidad Católica de Chile, Avenida Vicuña Mackenna 4860, Macul, Santiago, Chile.*

[5]*Facultad de Ciencias Químicas, Pontificia Universidad Católica de Chile.*

Abstract

We have studied the synthesis of palladium nanoparticles over carbon nanotubes (Pd/CNT) and graphene (Pd/G) and we have tested their catalytic performance in the liquid phase chemoselective hydrogenation of para-chloronitrobenzene at room temperature. The catalysts were characterized by N_2 adsorption/desorption isotherms, TEM, X-ray diffraction, infrared and X-ray photoelectron spectroscopy and ICP-OES. The palladium particle size on Pd/G (3.4 nm) and Pd/CNT (2.8 nm) was similar though the deposition was higher on Pd/G. Pd/CNT was more active which can be ascribed to the different surface area and electronic properties of the Pd nanoparticles over CNT, while the selectivity was 100% to the corresponding haloaniline over both catalysts and they were quite stable upon recycling.

Keywords: Carbon nanotubes; graphene; palladium; para-chloronitrobenzene; hydrogenation.

To whom correspondence should be addressed

**Dr.* A.B.Dongil*., e-mail:* adongil@udec.cl, *Tel: (56-41) 2207236.*

1. Introduction

The hydrogenation of halonitrocompounds has been traditionally performed by the Béchamp process. However, the increasing production of aromatic haloamines, which are extensively used as intermediates in the fine chemistry industry, requires the development of more environmentally friendly systems [1]. It has been reported that palladium and platinum offer good activities for this hydrogenation [1], but palladium is cheaper and more resistant to deactivation than platinum [2]. However, to achieve yields higher than 99 % of the desired aromatic haloamines it is necessary to add modifiers or to employ bimetallic catalysts [3,4]. Moreover, the use of a hydrophobic support as carbon materials may inhibit the formation of aniline [5,6]. In addition, the morphology of carbon nanotubes as rolling graphene layers might influence the adsorption of the molecules and hence the catalytic performance. Besides, their particular electronic properties can induce a positive charge on the metal species due to electron transfer [7], this activating the N=O bond. However, to obtain an optimal size of the nanoparticles a previous oxidation step is frequently needed which may affect the catalytic performance [6]. Therefore alternative methods to synthetize metal nanoparticles have to be developed. The synthesis of heterogeneous catalysts by deposition of pre-synthetized metal nanoparticles has been successfully employed for a variety of catalytic systems. In these systems the synthesis of the metal nanoparticles is performed by the decomposition of organometallic precursors under H_2 pressure and they are then deposited on the support to obtain a homogeneous particle size distribution [8,9]. On the

other hand, recent literature pointed to graphene oxide as an ideal candidate to support metal nanoparticles. The methods of synthesis of the nanoparticles may promote the reduction of graphene oxide, obtaining a more hydrophobic material compared to the parent graphene oxide [2,10].

Therefore, we have explored the synthesis of palladium nanoparticles over graphene and carbon nanotubes and we have tested their catalytic performance on the hydrogenation of p-chloronitrobenzene (p-ClNB).

2. Experimental

2.1 Catalysts synthesis

As received commercial carbon nanotubes (Nanocyl 3100, > 95% purity, CNT) and a lab-prepared graphite oxide (GO) following a modification of the Brodie´s method [11] were used as starting material. Two catalysts of 1 % wt. of Pd loading were prepared according to the following procedure: 4.3 mg of $Pd_2(dba)_3$ (dba: dibenzylidenacetone) per gram of support was dispersed in 40 ml of tetrahydrofuran THF and submitted to 3 bar of H_2 pressure for 24 h to obtain Pd nanoparticles. Then, the supports, CNT and GO, were suspended in 40 ml of THF along with the previously synthetized Pd nanoparticles and the mixture was submitted to 3 bar of hydrogen for 24 h. Finally, the solids were recovered and extensively washed with acetone in a rotatory evaporator and dried under vacuum at 323 K for 16 h. The catalysts were denoted as Pd/CNT and Pd/G.

2.2 Characterization

The textural properties of the materials were determined by N_2 adsorption at 77 K on a Micromeritics ASAP 2010 apparatus. X-ray powder diffraction patterns were recorded on a Rigaku diffractometer equipped with a nickel-filtered CuKα1 radiation (λ=

1.5418˚A), using a $2^{o}\cdot min^{-1}$ scanning rate and $1^{o}\cdot min^{-1}$ for the 35-45 º region. TEM images were taken with a JEOL electron microscope (model JEM-2010) working at 200 kV and it was equipped with an INCA Energy TEM 100 analytical system and a SIS MegaView II camera. 200 nanoparticles were measured to estimate the average particle size. The surface acidity of calcined samples was measured by potentiometric titration of a suspension of the catalyst in acetonitrile with n-butylamine, using an Ag/AgCl electrode [12].

Infrared spectra were collected by using a NicoletNexus FT-IR in the middle range (4000–400 cm^{-1}) and recorded by a DTGS detector from 128 scans and with a resolution of 4 cm^{-1}. The samples were mixed with predried potassium bromide to a final concentration of approximately 1% (w/w).

The actual metal loading of Pd on the different catalysts was determined by ICP-OES in a Perkin–Elmer device (Optimal 3000). The metal was extracted from the catalysts by digestion in HNO_3/H_2O_2 (4:1) for 30 min, in a microwave oven at 473 K. X-Ray photoelectron spectroscopy (XPS) analyses were performed with a VG Escalab 200R spectrometer equipped with a hemispherical electron analyzer and a Mg-Kα (h = 1253.6 eV; 1 eV = 1.6302·10-19 J) X-ray source operated at 10 mA and 12 kV.

2.3 Hydrogenation reaction

Catalytic tests were performed in a stainless steel Parr-type batch reactor, equipped with a glass sleeve and a magnetic stirrer set at 1000 rpm. The hydrogenations were performed with 50 mg of catalyst, 320 mg of p-chloronitrobenzene and 50 mL of ethanol at 20 bar and 298 K. For the recycling studies the catalysts were recovered by filtration and dried under vacuum. The amounts of p-ClNB, and ethanol were recalculated according to the recovered mass of catalyst to preserve the initial

concentration and S/C ratio. Details on the analyses of reactants and products can be found elsewhere [6]. Additional experiments were performed to verify that the reaction was heterogeneously catalyzed: the reaction was stopped at 50% conversion and the liquid filtrate was submitted to the reaction conditions.

3. Results

3.1 Characterization

Representative TEM images of the catalysts are shown in Fig. 1. They show that palladium nanoparticles were homogeneously distributed on the surface of CNT and G supports with a narrow size distribution, as can observed in the histograms. The average particle size was similar and the values, in Table 1, were 2.8 and 3.4 nm for Pd/CNT and Pd/G respectively which are in the range of values previously reported in literature for Pd nanoparticles over graphene and graphene oxide [13,14], and slightly smaller than non-supported palladium nanoparticles stabilized by an organic moiety [9]. Moreover, the TEM images showed that the Pd/G catalyst presented transparent areas corresponding to exfoliated graphene sheets.

The XRD patterns of GO and the Pd/G catalyst are shown in Fig. 2. For the sample GO the intense and sharp peak of the (001) reflection centered at $2\theta=15.4°$ corresponding to an interlayer distance of 0.57 nm, together with the disappearance of the peak at 26º due to the reflection of the (002) plane of graphite confirms a high yield in the GO synthesis [15]. On the other hand, the characteristic peak of GO disappeared for the sample Pd/G and only a less intense and broad peak at 2θ ~26° is insinuated which may be due to the presence of multilayer graphene [10], in agreement with the TEM images. The XRD of CNT support and the Pd/CNT catalyst (not shown) displayed the characteristic peak of graphite at 2θ = 26º. In order to check the existence of the characteristic peaks of

palladium, the 35-45º region was analyzed with a lower scan rate. The patterns, in Fig. S1, showed a very small peak at 40º corresponding to the (111) reflection of Pd^0 probably because of the low percentage of metal on the samples and/or to the small particle size, which would suggest a high Pd dispersion on the supports.

The acid strength and total acidity of the supports is summarized in Table 2. According to the criterion proposed in the literature [12], the CNT and Pd/CNT samples have very weak acid sites (E_0 < -100 mV), while the GO support has very strong acid sites (E_0 > 100 mV). However, the catalyst Pd/G displayed weak acid sites (0 < E_0 < -100 mV), this suggesting that it has lost the acidity of the parent GO support during the synthesis process, which might be due to the use of vacuum [16].

Infrared spectra of GO and Pd/G are shown in the supplementary information, Fig. S2. GO displayed the characteristic bands of C-OH groups at 3600, 3400, 1620 and 1383 cm^1 [15,17], C=O bond of carbonyl and/or carboxyl while band at 1730 cm^{-1} and the band at 1063 cm^{-1} due to the deformation of the C-O bond of epoxy functionalities. For the sample Pd/G a clear decrease of the intensity of the band at 3400 cm^{-1}, the presence of a band at 1578 cm^{-1} ascribed to the vibration of Csp2-Csp2 bonds characteristic of the skeletal vibrations of graphitic domains and some qualitative changes in the low frequency range confirm the partial reduction of this material.

Analyses of the XPS spectra of the supports and the catalysts were performed and the C1s and O1s levels are shown in Fig.3a and 3b respectively. As expected, the position of the maximum of the C1s spectra for GO appears at higher B.E, 286.0 eV, than the corresponding to graphite, i.e. 284.6 eV, and the characteristic $\pi \rightarrow \pi^*$ peak of polyaromatic structures is absent. This confirms that the main contribution is associated to defects. For the Pd/G catalyst the contribution of Csp3 at 286.0 eV has clearly decreased, the new maximun being 284.6 eV. This indicates that the material recovered

the aromaticity to some extent as the infrared spectra and XRD results suggested. The detailed B.E. values for the C 1s and O 1s regions along with their proportions, which are in agreement with literature [15, 18], are included in the supporting information (see Table S1). In addition, it can be observed in Table 1 that the O/C ratio decreases for the Pd/G catalyst but it increases for Pd/CNT compared to their corresponding supports. For the Pd/CNT catalyst this can be explained by the presence of adsorbed organic moieties on the surface of the catalysts as schematized in Fig. S3. For Pd/G, the decrease of the O/C ratio would confirm that the concentrations of the oxygen groups of the parent GO has decreased in agreement with the infrared and potentiometric results, although the presence of adsorbed organic moieties cannot be excluded.

Moreover, both catalysts displayed a new peak in the 335 eV region, in Fig 4, corresponding to the Pd $3d_{5/2}$ transition and the BEs values are shown in Table 1. Interestingly the deconvolution of this region displayed only one contribution ascribed to Pd^0, i.e. 335 eV [19], for both catalysts, despite the mild conditions employed for the synthesis of the nanoparticles. The higher B.E. observed for Pd/CNT could be ascribed to the presence of partially positively charged Pd nanoparticles on this catalyst. The Pd/C ratio was also estimated and the values, which are reported in Table 1, showed that the Pd/C ratio for Pd/G was higher than that of Pd/CNT in agreement with the results obtained by ICP-OES (Table 1).

3.3 Hydrogenation of p-ClNB

The catalysts were tested on the liquid phase hydrogenation of p-chloronitrobenzene whose main reaction paths are shown in Scheme 1 [20]. The activity at 50% conversion was estimated and the values showed that the Pd/CNT catalyst was more active than Pd/G. The activity achieved with Pd/G was in the range of the values reported for 5.5.

nm Pd nanoparticles supported over activated carbon, while that obtained with Pd/CNT was nearly one order of magnitude higher [21]. As far as the selectivity is concerned, p-ClAN was the only product of the reaction detected for both catalysts and, under the experimental conditions employed, no intermediates were observed.

In addition, the stability was studied by recycling the catalysts in three cycles and the evolution of the conversion with time is shown in Fig. 5 a-b. It can be observed that the activity decreased in the second cycle for both catalysts, this decrease being slightly more pronounced for Pd/CNT (26%) than for Pd/G (21 %) catalyst. However, the activity was constant in the third cycle for both catalysts. Furthermore, the selectivity to p-ClAN remained 100% upon recycling. Additional experiments described in the Experimental Section were performed with the catalysts to verify the possibility of leaching of palladium nanoparticles, which could homogenously catalyse the reaction. The absence of reaction with the liquid filtrate on those experiments confirmed that the reaction was heterogeneously catalysed.

The higher intrinsic activity achieved with the Pd/CNT catalyst might be related to the higher surface area of Pd/CNT catalyst, though the improved activation of the N=O bond due to the presence of $Pd^{+\delta}$ species cannot be excluded [22]. On the other hand, the excellent selectivity achieved with both catalysts can be explained by the hydrophobic nature of the support as previously suggested for other carbon materials [5]. It seems that the inert surface may avoid the adsorption of the formed p-ClAN as the π-cloud of the support is able to repel the chlorine atom moiety [5,23,24]. In this sense, the characterization results showed that Pd/G catalyst has a lower concentration of oxygen groups compared to GO material, and that it has partially recovered the graphitic character, this favoring the selectivity to the p-ClAN molecule and suggesting that the remaining oxygen groups do not affect the selectivity.

Finally the catalysts proved to be stable upon recycling. After the loss of activity in the second cycle, probably due to the leaching of adsorbed palladium nanoparticles as the XPS results suggested, the activity was constant and, according to the estimated particle size in Table 1, the nanoparticles did not suffer agglomeration upon recycling.

Conclusions

We have synthetized Pd nanoparticles over CNT and graphene and compared their catalytic performance on the chemoselective hydrogenation of p-ClNB. The characterization results showed that the method of synthesis was effective for obtaining metal palladium nanoparticles of similar size on Pd/CNT and Pd/G, although the yield of palladium deposition was higher on the Pd/G catalyst. This seems to indicate that the particle size was not affected by the morphology or the surface chemistry. The Pd/CNT catalyst was more active than Pd/G, which could be ascribed to the higher surface area or to the presence of partially positively charged Pd nanoparticles, and the selectivity to p-ClAN was 100% over both catalysts, what has been attributed to their hydrophobic surface. Finally, both catalysts were very stable upon recycling although some loss of activity was observed after the first cycle which could be ascribed to a certain leaching of the active phase.

Acknowledgments

Financial support for the present study was received from CONICYT Chile, project 3130483 (Postdoctoral), Generalitat Valenciana, Spain (PROMETEOII/2014/004) is also gratefully acknowledged.

5. References

Figure. 1 TEM micrographs and histograms of a, b) Pd/G and c,d) Pd/CNT. Scale bar: 10 nm.

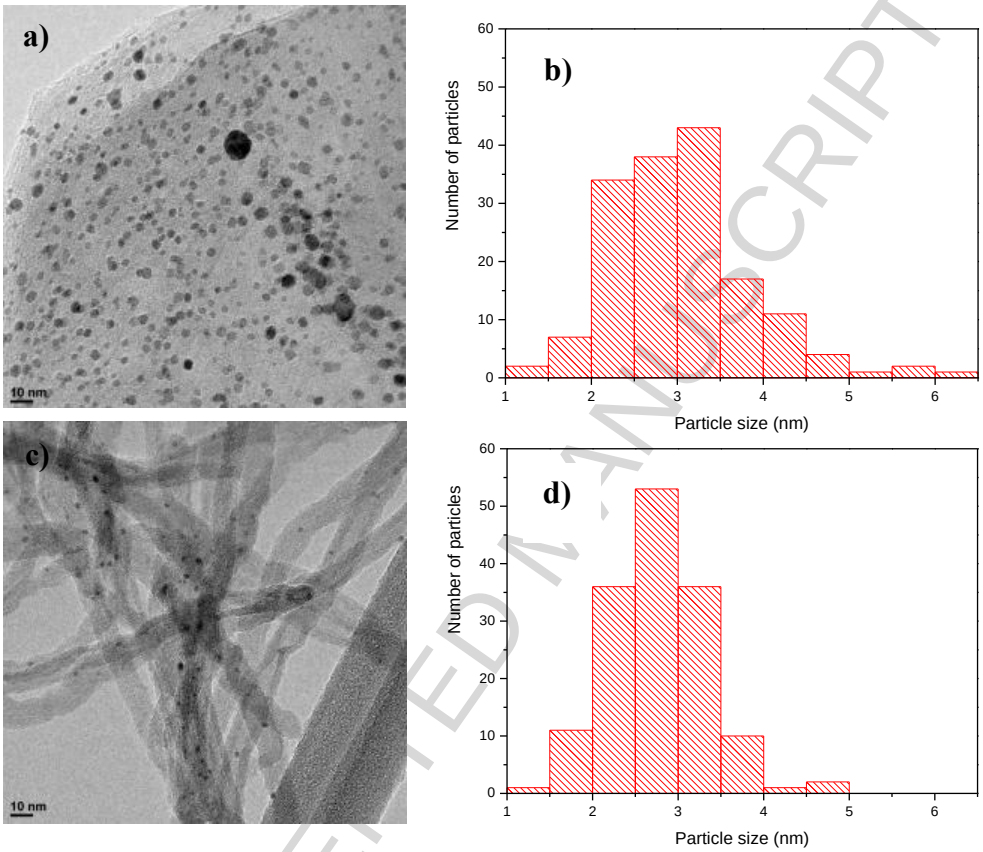

Figure 2. XRD patterns of graphite, GO and Pd/G.

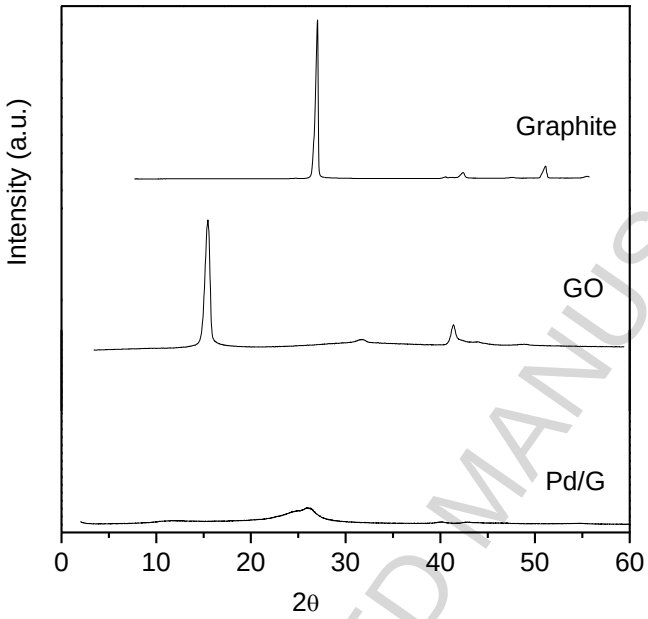

Figure 3. XPS spectra of the supports and the catalysts: a) C 1s, b) O1s.

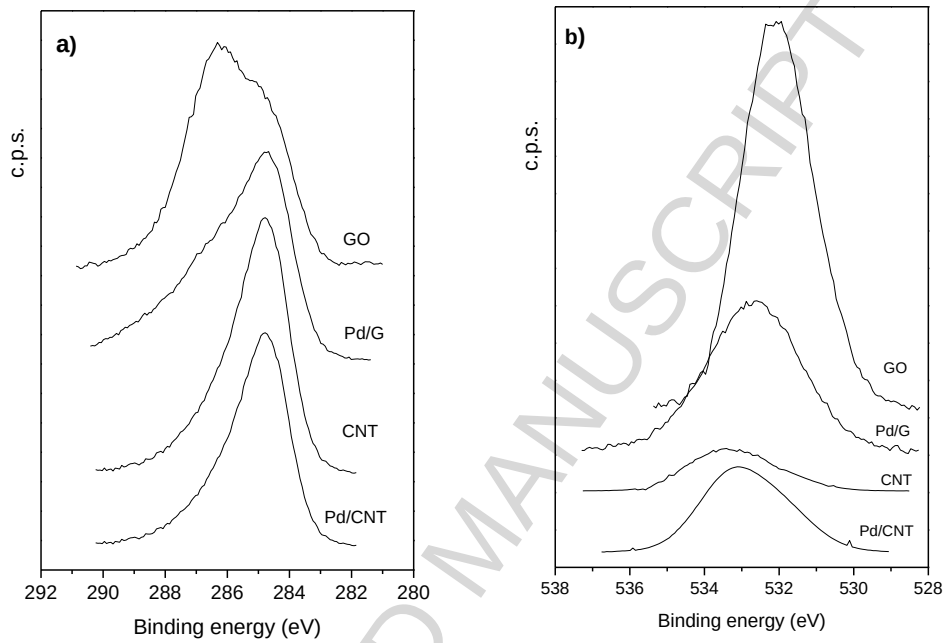

Figure 4. XPS spectra of the Pd 3d region of the fresh catalysts a) Pd/G and b) Pd/CNT.

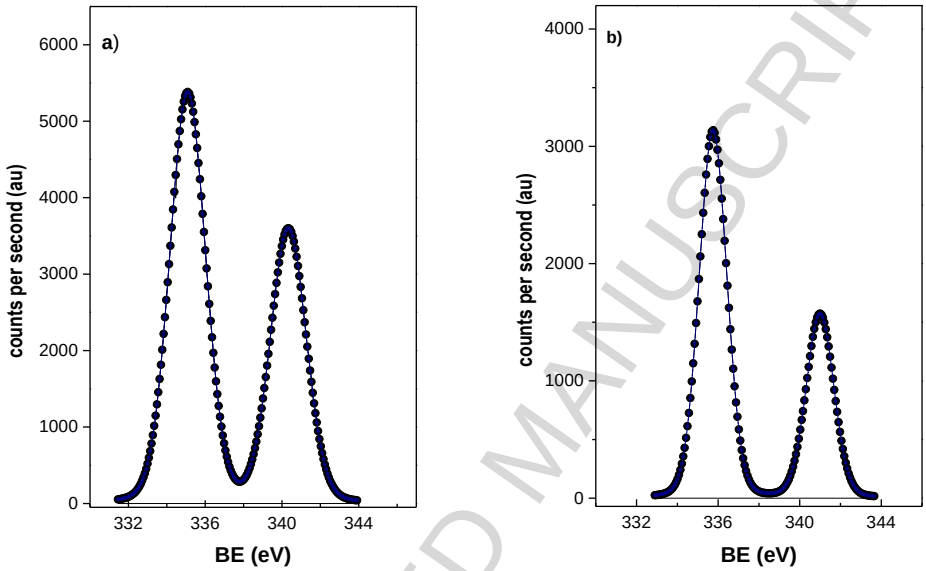

Scheme 1. Reaction paths for the para-chloronitrobenzene hydrogenation.

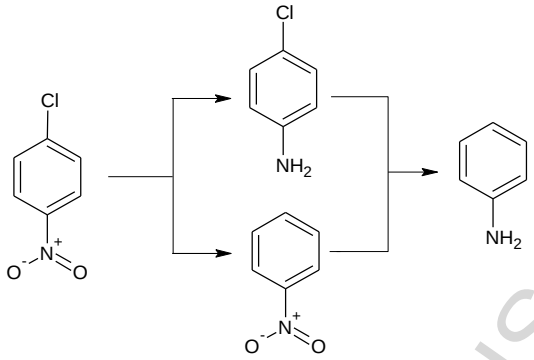

Figure 5. Conversion of p-cloronitrobenzene *versus* time over a) Pd/CNT and b) Pd/G on successive cycles.

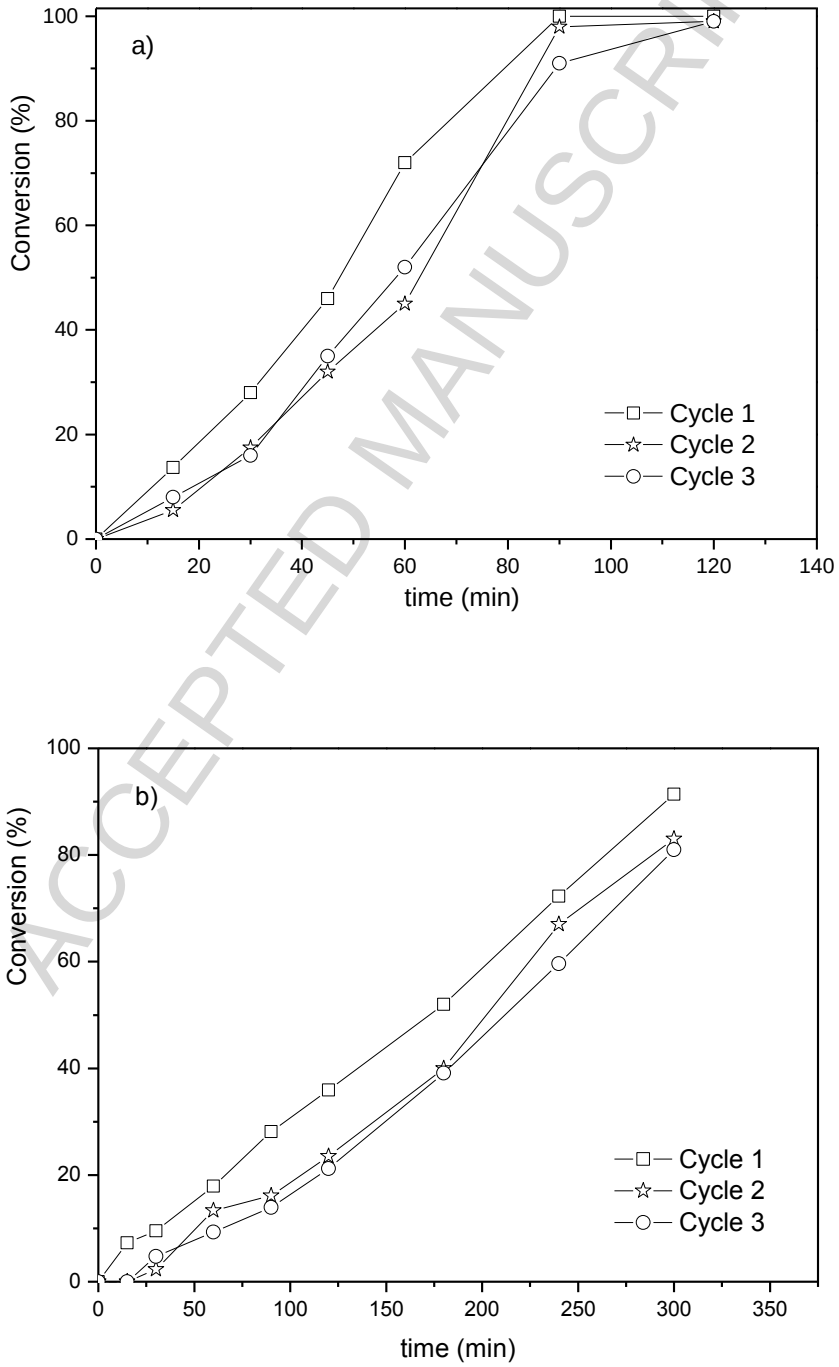

Table 1. Physico-chemical properties of the catalysts.

Sample	**S_{BET}(m^2/g)**	**Pd $3d_{5/2}$ eV**	**O/C at**	**Pd/C at**	**Pd (%) $_{ICP}$**	**dp TEM (nm)**
GO	-	-	0.355	-	-	-
CNT	300	-	0.011	-	-	-
Pd/G	36	335.0	0.181	0.010	0.71	3.4 ± 0.5
Pd/G- used	-	335.2	0.060	0.006	-	3.6 ± 0.5
Pd/CNT	288	335.6	0.072	0.004	0.50	2.8 ± 0.6
Pd/CNT- used	-	335.1	0.047	0.002	-	3.1 ± 0.5

Table 2. Acid strength of the supports and the catalysts.

Sample	Acid strength (mV)	Total acidity (meq/g)
CNT	-177	0.08
GO	360	0.59
Pd/CNT	-152	0.08
Pd/G	-31	0.56

Table 3. Hydrogenation of p-ClNB

Sample	Cycle	Activity (mol $_{p\text{-ClNB}}$ • mol_{Pd}^{-1} • min^{-1})[a]	time (min) 100% conv.	Yield to p-ClAN (%) at 100% conversion.
Pd/G	1	43	>300	100
	2	33	>300	100
	3	33	>300	100
Pd/CNT	1	190	90	100
	2	140	90	100
	3	140	120	100

Reaction conditions: ethanol, 20 bar, 298 K, S/C nominal=400, $[C_{p\text{-ClNB}}]$ t_0= 0.04 M.
[a] Intrinsic activity= Activity/Dispersion; Activity= mol of p-ClNB converted per mol of Pd (from ICP analyses) and reaction time for 50% conversion; Dispersion $_{Pd}$= $1.12/d_p$.

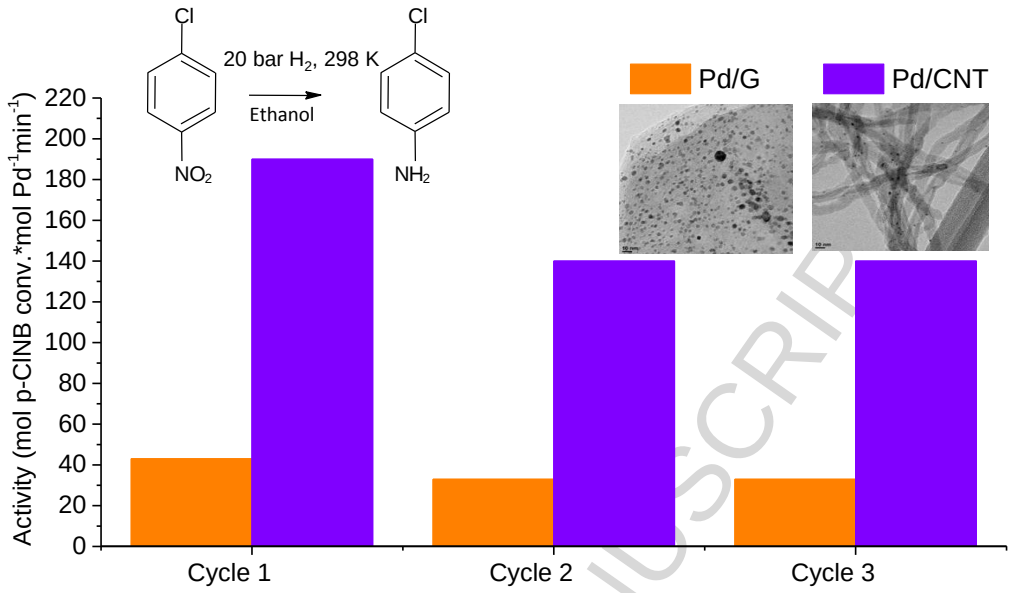

Graphical abstract

Highlights

- Pd nanoparticles were synthetized over carbon nanotubes and graphene by reduction of $Pd_2(dba)_3$.
- Well-dispersed metallic palladium nanoparticles of similar size were obtained over CNT and graphene.
- The catalyst Pd/CNT displayed better activity than Pd/G on the p-ClNB hydrogenation.
- The selectivity to p-ClAN was 100% with both catalysts.
- The catalysts Pd/CNT and Pd/G displayed good recyclability behavior.

[1] H.U. Blaser, A. Schnyder, H. Steiner, F. Rössler, P. Baumeister in Handbook of Heterogeneous Catalysis (Wiley, 2008), vol. 8 pp. 3284-3307.

[2] X. Chen, G.Wu, J.Chen, X. Chen, Z. Xie, X. Wang, J.Am.Chem.Soc. 133 (2011) 3693–3695.

[3] Q.Xu, X.M. Liu, J.R.Chen, R.X.Li, X.J. Li, J. Mol. Catal. A: Chemical 260 (2006) 299–305.

[4] F. Cárdenas-Lizana, S.Gómez-Quero, M.A. Keane, Catal. Comm. 9 (2008) 475–481.

[5] V. Kratky, M. Kralik, M. Mecarova, M. Stolcova, L. Zalibera, M. Hronec, Appl. Catal. A: General 235 (2002) 225–231.

[6] A.B. Dongil, C. Rivera-Cárcamo, L. Pastor-Pérez, A. Sepúlveda-Escribano, P. Reyes, Cat.Today, 249 (2015) 72-78.

[7] J.M. Nhut, L. Pesant, J.P. Tessonnier, G.Winé, J. Guille, C. Pham-Huu, M.J Ledoux, Appl. Catal. A: Gen. 254 (2003) 345–363.

[8] A Gual, C. Godard, K. Philippot, B. Chaudret, A. Denicourt-Nowicki, A. Roucoux, S. Castillón, C. Claver, ChemSusChem. 2 (2009) 769 - 779.

[9] S.Jansat, M. Gómez , K. Philippot , G. Muller , E.Guiu ,C. Claver, S.Castillón, B.Chaudret, J. Am. Chem. Soc., 126 (2004) 1592–1593.

[10] A.R. Siamaki, A.S. Khder, V. Abdelsayed, M.Shall, B. F.Gupton, J. Catal. 279 (2011) 1–11.

[11] A.B.Dongil, B.Bachiller-Baeza, A. Guerrero-Ruiz, I.Rodríguez-Ramos, Catal. Comm. 26 (2012) 149-154.

[12] R. Cid, G. Pecchi, Appl. Catal. 14 (1985) 15-21.

[13] W.Sun, X.Lu, Y.Tong, Z.Zhang, J. Lei, G.Nie, C.Wang, Int J. Hydrogen Energy 39 (2014) 9080–9086.

[14] K.H.Lee, S.W.Han, K.Y. Kwon, J. B. Park, J. Coll. Interf. Sci 403 (2013) 127–133.

[15] A.B. Dongil, B. Bachiller-Baeza, A. Guerrero-Ruiz, I. Rodríguez-Ramos, J. Catal. 282 (2011) 299-309.

[16] H.B. Zhang, J.W. Wang, Q.Yan, W.G. Zheng, C. Chen, Z. Z. Yu, J. Mater. Chem., 21 (2011) 5392-5397.

[17] T. Szabó, O. Berkesi, P. Forgó, K. Josepovits, Y. Sanakis, D. Petridis, and I. Dékény, Chem. Mater. 18 (2006) 2740.

[18] N.I.Kovtyukhova, P.J. Olliver, B.R. Martin, T.E. Mallouk, S.A. Chizhik, E.V. Buzaneva, A.D. Gorchinskiy, Chem. Mater. 11 (1998) 771-778.

[19] K. McEleney, C. M. Crudden, J. H. Horton, J. Phys. Chem. C, 113 (2009) 1901-1907.

[20] F. Cárdenas-Lizana, S. Gómez-Quero, C. Amorim, M.A. Keane, Appl. Catal., A: Gen., 473 (2014) 41–50.

[21] F. Cárdenas- Lizana, Y. Hao, M.Crespo-Quesada, I.Yuranov, X.Wang, M. A. Keane, L. Kiwi-Minsker, ACS Catal 3 (2013) 1386-1396.

[22] B. Zuo, Y. Wang, Q. Wang, J. Zhang, N. Wu, L. Peng, L. Gui, X. Wang, R. Wang, D. Yu, J. Catal. 222 (2004) 493-498.

[23] J.P. Tessonnier, L. Pesant, G. Ehret, M. J. Ledoux, C. P.Huu, Appl. Catal. A: General 288 (2005) 203–210.

[24] N. Mahata, A.F. Cunha, J.J.M. Órfão, J.L. Figueiredo, Catal. Comm 10 (2009) 1203-1206.